Original Investigation

Evolution of Diffusion-Weighted Magnetic Resonance Imaging Signal Abnormality in Sporadic Creutzfeldt-Jakob Disease, With Histopathological Correlation

Laura Eisenmenger, MD; Marie-Claire Porter, MD; Christopher J. Carswell, PhD; Andrew Thompson, PhD; Simon Mead, PhD; Peter Rudge, FRCP; John Collinge, FRS; Sebastian Brandner, MD, FRCPath; Hans R. Jäger, MD, FRCR; Harpreet Hyare, PhD

IMPORTANCE Prion diseases represent the archetype of brain diseases caused by protein misfolding, with the most common subtype being sporadic Creutzfeldt-Jakob disease (sCJD), a rapidly progressive dementia. Diffusion-weighted imaging (DWI) has emerged as the most sensitive magnetic resonance imaging (MRI) sequence for the diagnosis of sCJD, but few studies have assessed the evolution of MRI signal as the disease progresses.

OBJECTIVES To assess the natural history of the MRI signal abnormalities on DWI in sCJD to improve our understanding of the pathogenesis and to investigate the potential of DWI as a biomarker of disease progression, with histopathological correlation.

DESIGN, SETTING, AND PARTICIPANTS Gray matter involvement on DWI was assessed among 37 patients with sCJD in 26 cortical and 5 subcortical subdivisions per hemisphere using a semiquantitative scoring system of 0 to 2 at baseline and follow-up. A total brain score was calculated as the summed scores in the individual regions. In 7 patients, serial mean diffusivity measurements were obtained. Age at baseline MRI, disease duration, atrophy, codon 129 methionine valine polymorphism, Medical Research Council Rating Scale score, and histopathological findings were documented. The study setting was the National Prion Clinic, London, England. All participants had a probable or definite diagnosis of sCJD and had at least 2 MRI studies performed during the course of their illness. The study dates were October 1, 2008 to April 1, 2012. The dates of our analysis were January 19 to April 20, 2012.

MAIN OUTCOMES AND MEASURES Correlation of regional and total brain scores with disease duration.

RESULTS Among the 37 patients with sCJD in this study there was a significant increase in the number of regions demonstrating signal abnormality during the study period, with 59 of 62 regions showing increased signal intensity (SI) at follow-up, most substantially in the caudate and putamen ($P < .001$ for both). The increase in the mean (SD) total brain score from 30.2 (17.3) at baseline to 40.5 (20.6) at follow-up ($P = .001$) correlated with disease duration ($r = 0.47$, $P = .003$ at baseline and $r = 0.35$, $P = .03$ at follow-up), and the left frontal SI correlated with the degree of spongiosis ($r = 0.64$, $P = .047$). Decreased mean diffusivity in the left caudate at follow-up was seen ($P < .001$). Eight patients demonstrated decreased SI in cortical regions, including the left inferior temporal gyrus and the right lingual gyrus.

CONCLUSIONS AND RELEVANCE Magnetic resonance images in sCJD show increased extent and degree of SI on DWI that correlates with disease duration and the degree of spongiosis. Although cortical SI may fluctuate, increased basal ganglia SI is a consistent finding and is due to restricted diffusion. Diffusion-weighted imaging in the basal ganglia may provide a noninvasive biomarker in future therapeutic trials.

JAMA Neurol. 2016;73(1):76-84. doi:10.1001/jamaneurol.2015.3159
Published online November 16, 2015.

Supplemental content at jamaneurology.com

Author Affiliations: Department of Radiology, University of Utah, Salt Lake City (Eisenmenger); Medical Research Council Prion Unit, Department of Neurodegenerative Diseases, University College London Institute of Neurology, London, England (Porter, Carswell, Thompson, Mead, Rudge, Collinge, Brandner, Hyare); Lysholm Department of Neuroradiology, National Hospital for Neurology and Neurosurgery, London, England (Jäger).

Corresponding Author: Harpreet Hyare, PhD, Medical Research Council Prion Unit, Department of Neurodegenerative Diseases, University College London Institute of Neurology, Queen Square, London, WC1N 3BG, England (harpreet.hyare@nhs.net).

Diffusion-weighted imaging (DWI) has emerged as the most sensitive magnetic resonance imaging (MRI) sequence in the diagnosis of sporadic Creutzfeldt-Jakob disease (sCJD),[1-3] with studies[4-6] showing its superiority for detecting signal change in the cortex. Visual inspection of the trace-weighted diffusion image demonstrates typically increased signal intensity (SI) in the cortex, with up to 95% of cases showing hyperintensity affecting the insula, cingulate, and superior frontal cortex independent of deep gray matter involvement.[3] The extent of involvement and the distribution of signal changes vary among patients and are thought to be influenced by *PRNP* (OMIM 123400) genotype and strain type of the abnormal isoform of the prion protein.[7,8] However, few studies[9,10] have assessed the evolution of these signal abnormalities as sCJD progresses.

In the largest series to date of 8 patients with CJD having serial DWI, there was progression or constant lesion distribution, with increased SI in some lesions and decreased SI in others.[9] In 5 of 8 patients, a defined temporal sequence of events was reported in which a high signal starts in the anteroinferior putamen and spreads to its posterior part, leading to complete involvement of the putamen. Another study[10] describes the initial expansion of the signal changes but resolution of the cortical signal change, with general progression to cerebral atrophy at later stages of CJD, and 2 other studies[11,12] report the disappearance of diffusion signal changes at terminal stages of the disease.

The objective of this study was to assess the natural history of the MRI signal abnormalities on DWI in patients with sCJD to better understand the pathogenesis of the disease and to develop a noninvasive measure of disease progression for future therapeutic trials. Our hypothesis was that the extent and degree of SI increases with sCJD progression.

Methods

Participants

The study setting was the National Prion Clinic, London, England. In 2004, the chief medical officer wrote to UK neurologists, requesting that all patients with suspected CJD are referred to both the National CJD Research and Surveillance Unit in Edinburgh, Scotland, and the National Prion Clinic based at the National Hospital for Neurology and Neurosurgery in London. Magnetic resonance images of all patients seen are sent to the National Prion Clinic in digital format. The MRIs studied herein came from patients who were referred to the National Prion Clinic by their local physician between October 1, 2008, and April 1, 2012, with full written informed consent, and the patients were enrolled into either the PRION-1 clinical trial[13] or the ongoing National Prion Monitoring Cohort study.[14] Both studies were approved by the Eastern Medical Research Ethics Committee, London, and are compliant with the Declaration of Helsinki.

We identified 37 consecutive participants with sCJD in whom at least 2 serial MRI studies had been performed during the course of their illness, with the inclusion of a DWI sequence at each study. The mean age at baseline MRI of the participants was 65.3 years (age range, 39-85 years), and 14 were female. In 4 participants in whom multiple serial MRI studies were obtained (3, 3, 3, and 4 studies, respectively), only the initial baseline and the last available follow-up MRI scans were included for analysis. The mean time between MRI studies was 3.6 months (range, 0.5-29 months). Thirty patients had their MRI studies performed at the referring hospital, and 7 patients had their MRI studies performed at the National Hospital for Neurology and Neurosurgery, London. All external DWI studies were performed at 1.5 or 3 T, with a b value of 1000 s/mm^2. Slight differences in section thickness were seen, varying from 3 to 5 mm. The mean disease duration at the initial MRI was 5.7 months. All patients had a clinical diagnosis of sCJD based on the proposed World Health Organization classification,[15] confirmed by postmortem examination in 21 of 37 patients (57%). Details of the autopsy findings are listed in eTable 1 in the Supplement. The remaining cases were diagnosed as probable sCJD according to accepted diagnostic criteria.[15] In all participants, age at baseline MRI, disease duration, *PRNP* mutation analysis, codon 129 methionine valine (MV) polymorphism, and clinical evaluation with the Medical Research Council Rating Scale[14] were documented.

MRI Acquisition

Seven patients underwent imaging at our institution, 3 on a 3-T MRI system (Tim Trio; Siemens) and 4 on a 1.5-T MRI system (Signa LX; GE). For these patients, both baseline and follow-up MRI studies were performed on the same MRI system. The 3-T diffusion-tensor imaging sequence consisted of 75 sections of 2.0-mm thickness, with a b value of 1000 s/mm^2, in 64 noncolinear directions (repetition time/echo time of 9500/93 milliseconds, 19.2-cm field of view, 96 × 96-pixel matrix, and a mean of 1 signal), with 8 images having a b value of 0 s/mm^2. The diffusion trace-weighted image and the corresponding mean diffusivity (MD) map were generated by the imaging system. At 1.5 T, DWI was performed using a single-shot echoplanar technique (repetition time/echo time of 10 000/101 milliseconds, 26-cm field of view, 96 × 128-pixel matrix, 5-mm section thickness, and a mean of 1 signal), with diffusion-weighting factors (b values) of 0 and 1000 s/mm^2 applied sequentially along 3 orthogonal axes.

MRI Visual Assessment

Signal Intensity

Two neuroradiologists (reader 1 [H.H.] with 9 years of experience in prion imaging and reader 2 [R.J.] with 25 years of experience in prion imaging) independently reviewed all MRI sequences. The readers were aware of the clinical diagnosis of sCJD in all patients, either confirmed after death or classified as probable cases according to accepted diagnostic criteria.[15] All images were viewed digitally on a workstation (Picture Archiving and Communications System; Agfa) with facilities for appropriate windowing (adjustment of SI) and SI measurements. Any MRI studies performed externally were uploaded onto our in-house workstation and were windowed to appear as similar as possible. Gray matter involvement on the diffusion-weighted trace image was reported in 26 cortical and

5 subcortical subdivisions per hemisphere.[16] If a discrepancy was identified, the images were rereviewed in a consensus reading. A κ statistic was calculated to assess the level of agreement between the 2 independent readers.

We used a semiquantitative scoring system that was devised on 5 test cases by drawing a region of interest in normal-appearing white matter and comparing the mean SI in several cortical gray matter regions visually thought to be normal, mildly hyperintense, and clearly hyperintense. The semiquantitative scoring system was found to be robust. A score of 0 indicated normal, with the SI within 2 SDs of the white matter SI. A score of 1 indicated mildly hyperintense, with the SI greater than 2 SDs above the white matter SI but less than 2 times the white matter SI. A score of 2 indicated clearly hyperintense, with the SI at least 2 times the white matter SI (eFigure 1 in the Supplement). To distinguish artifactual cortical DWI hyperintensity from true cortical signal abnormality, the MD map was examined in conjunction with the DWI image to identify corresponding areas of hypointensity. A total brain score was calculated as the summed scores in the individual regions (31 regions per hemisphere), with the maximum total brain score being 124. The aim was to assess both the extent and intensity of signal abnormality in a particular MRI scan. A cortical score was calculated as the sum of all 52 cortical regions, and a subcortical score was calculated as the sum of 10 subcortical regions.

Volume Loss

Frontal lobe, temporal lobe, parietal lobe, and generalized cortical atrophy were individually assessed in each study according to established criteria.[17,18] A score of 0 indicated normal, 1 indicated mild atrophy, 2 indicated moderate atrophy, and 3 indicated severe atrophy.

Quantitative Assessment

Pixel-by-pixel MD maps were generated from the directionally averaged images with b values of 0 and 1000 s/mm^2 using the equation by Stejskal and Tanner [19] for MD calculation as follows: MD = −[Inverse(*S*1 / *S*2) / (*b*1 − *b*2)], where *S*1 and *S*2 are the SIs of diffusion-weighted images with b values of 0 s/mm^2 (*b*1) and 1000 s/mm^2 (*b*2), respectively. The mean MDs in 3 regions of interest were drawn on the left cerebral hemisphere of the axial *b*0 image in the head of the left caudate nucleus, left putamen, and frontal white matter (volume, 587-597 mm^3). The region of interest mean from each of the corresponding MD maps was recorded.

Statistical Analysis

To assess change in SI from baseline to follow-up in a particular anatomical area, the Wilcoxon signed rank test was used. Because 65 comparisons were performed, the *P* values were adjusted to $P \leq .001$ for statistical significance. To assess correlation of total brain scores with age at baseline MRI, disease duration, atrophy, and Medical Research Council Rating Scale score, a Spearman rank correlation was performed. Finally, to assess change in MD between baseline and follow-up, the Wilcoxon signed rank test was used.

Quantitative Histopathological Analysis

Of the patients who underwent autopsy, the left frontal lobe sections were acquired from 8 individuals for quantitative analysis of the degree of spongiosis, calculated as the number of vacuoles per centimeter squared. Before analysis, all slides were reviewed by an experienced neuropathologist. For quality control purposes, slides that were found to be of poor quality, such as those that were inadequately stained or damaged, were replaced with newly acquired ones.

The slides were scanned into a database (SlidePath; Leica) and then loaded into a work space (Tissue Studio; Definiens). A region of interest was manually selected that was free of artifact and then drawn. An analysis builder was used to perform the following functions: (1) define the magnification strength of ×10, (2) apply a background to tissue separation for the analysis to be confined purely to brain tissue, (3) select the layer of tissue being analyzed, (4) apply homogeneity and brightness thresholds, (5) select the stain being analyzed (eg, hematoxylin-eosin), and (6) apply a stain threshold. Objects above and below a specific contrast intensity could then be deselected from the analysis. The degree of spongiosis was correlated with disease duration at death and SI in the left frontal cortex on MRI using the Spearman rank correlation coefficient.

Results

Consensus Review

In the initial analysis, there was disagreement regarding 3 patients. The discrepancy was cortical region scores (κ statistic, 0.835). These images were rereviewed, and consensus agreement was reached.

Baseline Analysis

Anatomical Regions

The cortical region that most commonly showed signal abnormality in baseline studies (SI 1 or 2) was the posterior cingulate gyrus, with 67% (28 of 37) involvement on the left and 73% (27 of 37) involvement on the right (there was no significant difference between the left and the right). The next most commonly involved region was the anterior cingulate gyrus, with 68% (25 of 37) involvement on the left and 65% (24 of 37) involvement on the right, followed by the left superior frontal gyrus, which showed signal abnormality in 65% (24 of 37) of patients. The area least likely to be involved was the hippocampus and amygdala. The mean (SD) number of anatomical regions involved at baseline was 21.8 (10.76) among 62 regions, with slight asymmetry that was not significant (mean [SD], 11.19 [5.79] regions in the left hemisphere and 10.59 [6.33] regions in the right hemisphere) (**Figure 1**).

Signal Intensity

The greatest SI in baseline studies was seen in the anterior cingulate gyrus (mean [SD], 1.00 [0.78] on the left and 1.00 [0.85] on the right) and the posterior cingulate gyrus (mean [SD], 0.95 [0.78] on the left and 0.95 [0.85] on the right), followed by the caudate nucleus (mean [SD], 0.89

Figure 1. Anatomical Distribution of Diffusion-Weighted Imaging Signal Intensity at Baseline and Follow-up

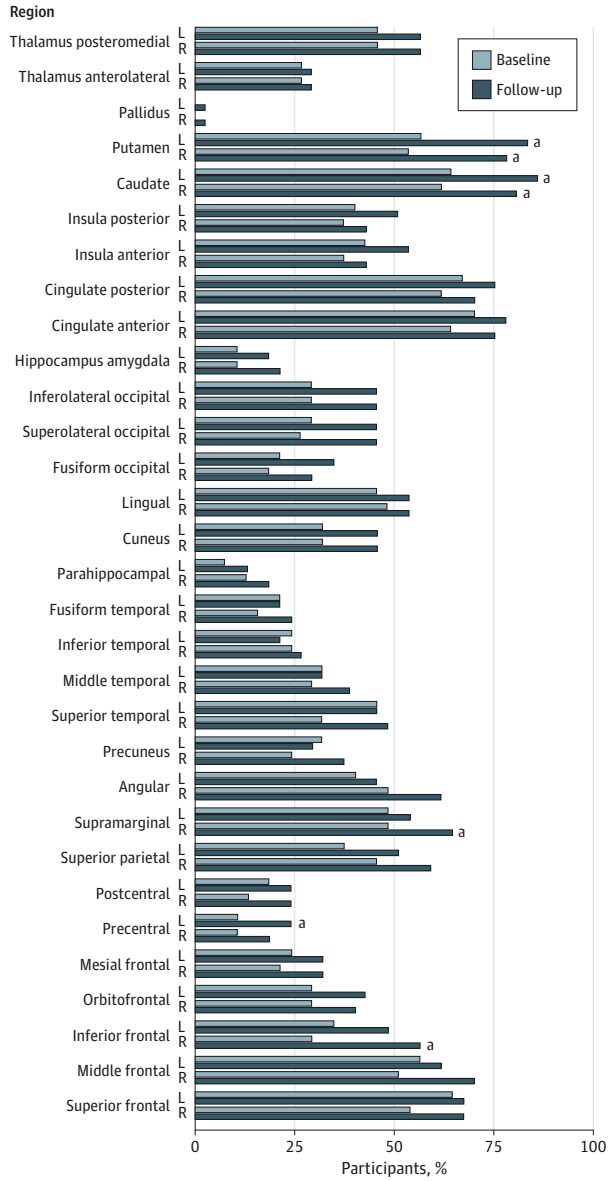

Shown are percentages of participants with diffusion-weighted imaging signal intensity of 1 or 2 in each of 31 brain regions at baseline (light blue) and follow-up (dark blue). L indicates left; R, right.
[a]*P* < .05.

Figure 2. Average Signal Intensity in Each Region at Baseline and Follow-up

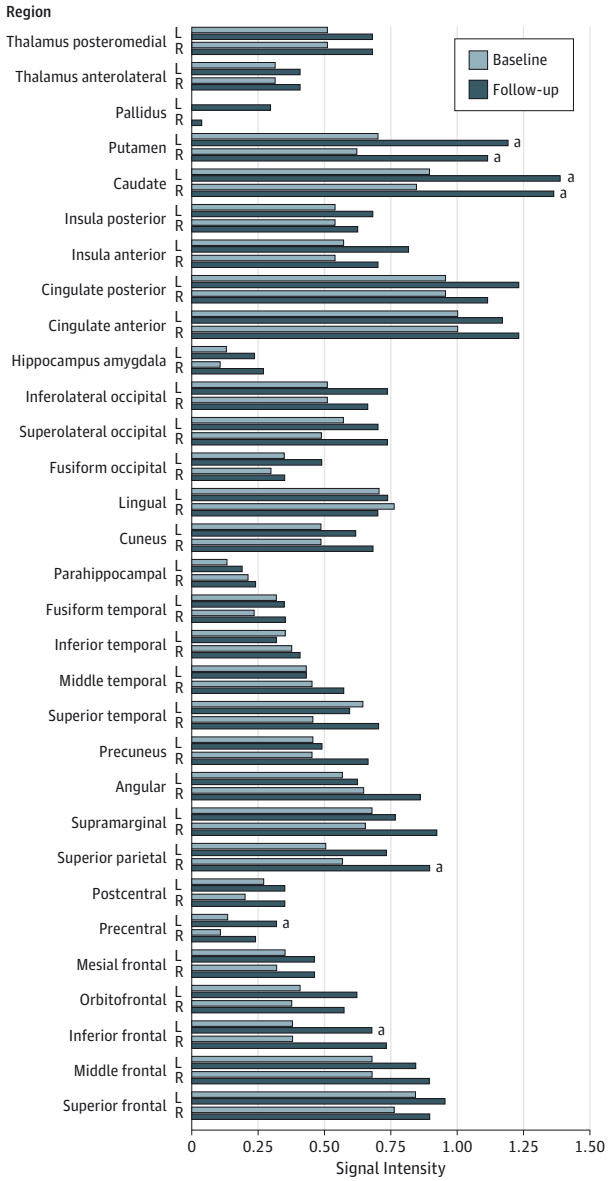

Shown is the mean signal intensity in each of 31 brain regions at baseline (light blue) and follow-up (dark blue). L indicates left; R, right.
[a]*P* < .05.

[0.77] on the left and 0.84 [0.76] on the right) and the left superior frontal gyrus (mean [SD], 0.84 [0.73]) (**Figure 2** and eTable 2 in the Supplement). The least SI was seen in the precentral gyrus, hippocampus and amygdala, and globus pallidus.

Volume Loss

Frontal volume loss was most often seen, with a mean (SD) score of 0.89 (0.62), followed by parietal volume loss, with a mean (SD) score of 0.76 (0.89). The mean (SD) global atrophy score of 0.54 (0.77) was next most common type, with mesiotemporal lobe atrophy rarely seen, having a mean (SD) score of 0.16 (0.55).

Follow-up MRI

Anatomical Regions

There was a significant increase in the mean (SD) number of anatomical regions demonstrating signal abnormality in follow-up studies, with 28.0 (12.6) vs 21.8 (10.8) at baseline (*P* = .001) and 13.8 (6.8) on the left (*P* = .004) and 14.2 (7.0) on the right (*P* < .001). **Figure 3**A-D shows the increase in the extent of cortical signal abnormality in follow-up studies.

Figure 3. Typical Examples of Change in the Extent and Intensity of Signal Abnormality on Diffusion-Weighted Imaging

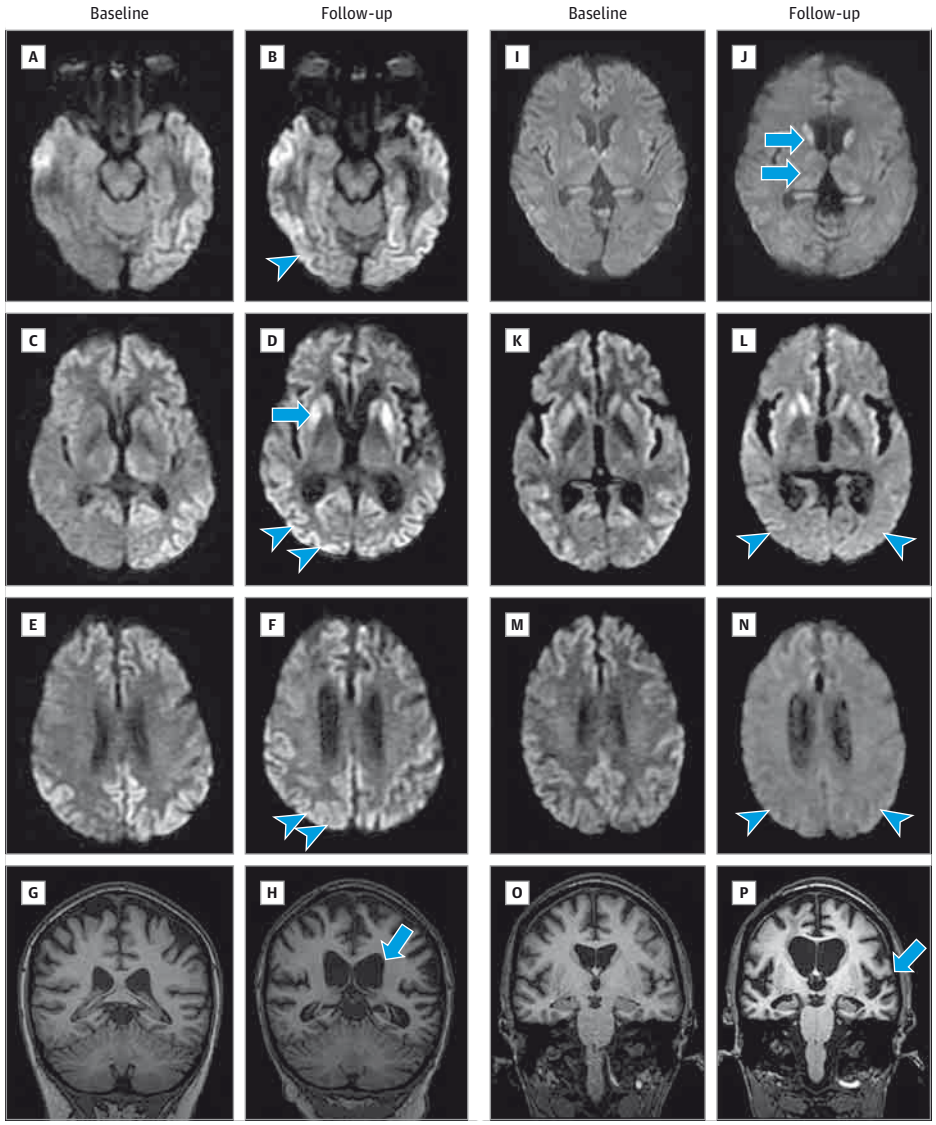

A-H, Shown are axial diffusion-weighted images in a 66-year-old woman with the codon 129 methionine valine polymorphism. A and B, The left temporo-occipital cortical signal abnormality (A) progresses to bilateral temporo-occipital cortical signal abnormality at follow-up 30 months later (arrowhead) (B). C and D, Signal intensity 0 in the right putamen at baseline (C) progresses to signal intensity 2 (arrowheads) and new right lateral occipital cortical signal abnormality at follow-up (arrow) (D). E and F, Bifrontal and biparietal cortical signal abnormality (E) progresses to increased right superior parietal cortical signal abnormality at follow-up (F). The arrowheads in F indicate increased right superior parietal signal abnormality. Note that the cortical signal abnormality progresses in contiguous cortical areas. G and H, Coronal T1-weighted images show progression of central and parietal atrophy from baseline (G) to follow-up (H). The arrow in H indicates increased central atrophy on follow-up. I and J, Axial diffusion-weighted images in a 60-year-old woman with the codon 129 valine homozygous polymorphism show an increase in caudate and thalamic signal intensity (arrows) from baseline (I) to follow-up 4 months later (J). K-P, Shown are axial diffusion-weighted images in a 53-year-old woman with the codon 129 methionine homozygous polymorphism. K-N, Baseline (K and M) and follow-up (L and N) axial diffusion-weighted images show decrease in cortical signal abnormality in the occipital lobes (arrowheads) at follow-up (L) compared with baseline (K) and decrease in cortical signal abnormality in the parietal lobes (arrowheads) at follow-up (N) compared with baseline (M). O and P, T1-weighted coronal images show progression of central and perisylvian atrophy (arrow) from baseline (O) to follow-up (P).

Signal Intensity

On average, 59 of 62 regions showed increased SI at follow-up. The regions that showed the greatest increase in SI were the caudate, with a mean (SD) of 0.89 (0.77) for baseline left vs 1.38 (0.72) for follow-up left and a mean (SD) of 0.84 (0.76) for baseline right vs 1.35 (0.77) for follow-up right ($P < .001$ for both) and the putamen, with a mean (SD) of 0.70 (0.71) for baseline left vs 1.19 (0.70) for follow-up left and a mean (SD) of 0.62 (0.64) for baseline right vs 1.11 (0.74) for follow-up right ($P < .001$ for both) (Figure 2 and eTable 2 in the Supplement). Examples of this increase in basal ganglia SI are shown in Figure 3D and J. The right inferior frontal gyrus showed the next largest increase in SI (Figure 2). The left middle temporal gyrus remained stable in SI at follow-up.

Volume Loss

There was an increase in all atrophy scores in follow-up studies, with a mean (SD) of 0.92 (0.76) for frontal, 0.76 (0.86) for global, 0.89 (0.97) for parietal, and 0.35 (0.72) for mesiotemporal. The most significant increase was found in global atrophy (P = .009). These results are shown in Figure 3H and P.

Total Brain Score

In total, 29 of 37 patients showed an increase in total brain score on follow-up MRI. On average, the mean (SD) total brain score increased from 30.2 (17.3) to 40.5 (20.6) (P = .001). This increase was due to an increase in the mean (SD) cortical SI, from 26.0 (19.1) to 35.3 (22.2) (P = .005) and in the mean (SD) subcortical SI from 4.5 (4.0) to 6.5 (4.3) (P = .008). There was a positive correlation between baseline (r = 0.47, P = .003) and follow-up (r = 0.35, P = .03) total brain score and disease duration (**Figure 4**) but no correlation between total brain score and age at baseline MRI, atrophy, and Medical Research Council Rating Scale score.

The remaining 8 patients showed a decrease in total brain score on follow-up study owing to a decrease in SI in cortical regions (from 35.1 to 25.0, a 29% decrease) but not in subcortical regions (from 2.8 to 5.9, a 53% increase) (Figure 3K-P). When we compared the patients who showed a decrease in total brain score with the patients who showed an increase in total brain score at follow-up, we found a slight increase in global atrophy scores (mean [SD], 0.79 [0.92] vs 0.71 [0.77]). We also found more patients with the codon 129 MV polymorphism (4 of 8 patients in the group that showed a decrease in total brain score had the codon 129 MV polymorphism compared with 7 of 29 patients in the group that showed an increase in total brain score.) Neither finding reached statistical significance. In addition, no significant difference was found in age at baseline MRI, disease duration, time to death, or Medical Research Council Rating Scale score.

Mean Diffusivity

In 7 patients who underwent imaging at our institution, serial MD measurements showed a significant decrease in MD in the left caudate and left putamen in follow-up studies compared with baseline studies (**Figure 5**). The mean (SD) left caudate MD was 646.1 (99.5) $\times 10^{-3}$ mm^2/s at baseline compared with 591.1 (89.7) 10^{-3} mm^2/s at follow-up (P < .001). The mean (SD) left putamen MD was 591.1 (123.6) 10^{-3} mm^2/s at baseline vs 531.2 (99.0) 10^{-3} mm^2/s at follow-up (P = .05). However, no significant difference was seen for frontal white matter.

Quantitative Histopathological Analysis

Clinical details of 8 patients who underwent quantitative histopathological analysis are listed in eTable 1 in the Supplement. There was a significant correlation between the left frontal MRI SI and the number of vacuoles per centimeter squared in the left frontal cortex (r = 0.64, P = .047) (eFigure 2A in the Supplement). There was also a significant correlation between disease duration at death and the number of vacuoles per centimeter squared in the left frontal cortex (r = 0.65, P = .04) (eFigure 2B in the Supplement).

Figure 4. Correlation of Total Brain Score With Disease Duration at Baseline and Follow-up

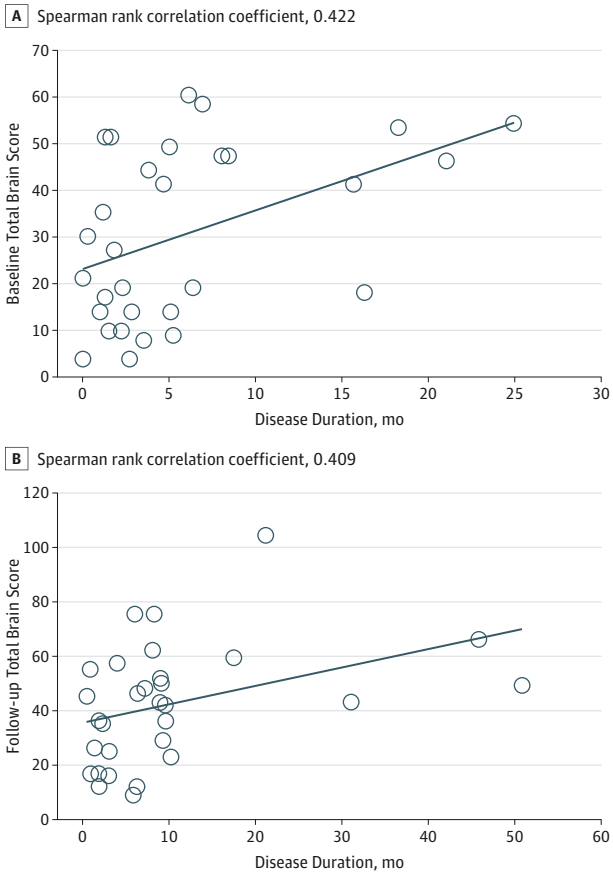

Scatterplots show positive correlation between baseline total brain score and disease duration and between follow-up total brain score and disease duration.

Discussion

To our knowledge, this study is the largest to date to describe the evolution of MRI signal abnormality on DWI in patients diagnosed as having sCJD, with histopathological correlation in a subgroup. We have shown that disease progression is accompanied by an increase in both the extent and intensity of signal abnormality. The basal ganglia showed a consistent and the most significant increase in SI as sCJD progresses. Measurements of MD performed in a subgroup showed that signal increase on the trace-weighted DWI images suggests restriction of water diffusion. In most patients with sCJD, disease progression is also associated with an increase in cortical signal abnormalities, which correlates with the degree of spongiosis. However, in some patients, we have seen a decrease in the extent and intensity of cortical signal abnormality, which is a potential pitfall of which physicians should be made aware.

Although the distribution of cortical and subcortical signal abnormality in sCJD has been well characterized in large cohorts,[2,4-6,16,20] few studies have examined the evolution of

Figure 5. Change in Basal Ganglia Mean Diffusivity Over Time

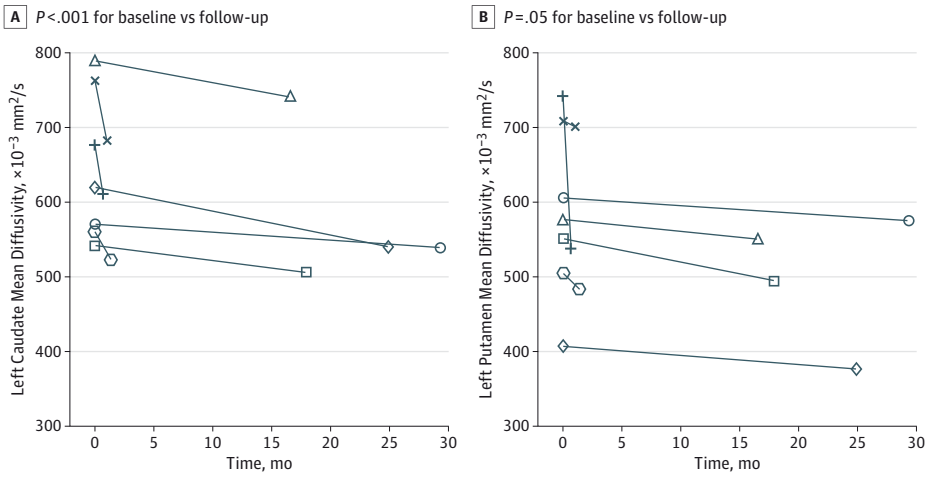

Symbols represent separate individuals.

signal abnormality in sCJD. In the largest series to date of 8 patients with serial imaging,[9] striatal involvement was seen in 7 of 8 patients in the final study. In another study[21] of serial MRI in 6 patients with sCJD, 3 of 5 patients with only cortical lesions seen on the initial study progressed to basal ganglia involvement and increased cortical involvement in the subsequent studies. In a single case report, increased basal ganglia and thalamic signal abnormality was seen on the third MRI at 9 months.[22] In our study, the caudate and putamen were the most commonly involved subcortical regions and showed the greatest SI on follow-up study.

Involvement of the thalamus and striatum is well established in sCJD.[23] The putamen and caudate nuclei receive input from diverse cortical areas, including prefrontal and limbic structures, with nonmotor output from the striatum projecting via the mediodorsal and ventrolateral thalamic nuclei to the dorsolateral prefrontal cortex, lateral orbitofrontal cortex, and anterior cingulate.[20] These subcortical structures appear to be increasingly involved as the disease progresses in sCJD, perhaps reflecting increased cortical involvement with disease duration as demonstrated in this study.

Diffusion-weighted imaging hyperintensity is thought to be owing to a combination of diffusion restriction and T2-weighted prolongation. Studies[12,24,25] that have measured MD in sCJD have shown decreased MD in the caudate, putamen, and thalamus. Longitudinal MD measurements in sCJD have demonstrated conflicting data, with one study[9] reporting decreased MD in the striatum during 2 weeks and other studies[12,26] reporting increased MD in the basal ganglia MD over time, suggesting that MD may vary according to the disease stage. We found a significant decrease in MD in the caudate and putamen at follow-up in our institution. Some changes in individual patients were modest, while other patients demonstrated more rapid change. Severe spongiform change, causing cell swelling and restricting the extracellular space, has been advocated as a potential cause of decreased MD,[27,28] and it is likely that increased spongiform degeneration as CJD progresses reduces MD in the subcortical structures even further.

The distribution of cortical signal abnormality in our study is in line with previous studies[2,3,16] reporting that the frontal, limbic, and parietal lobes are predominantly involved, with relative sparing of the precentral and central gyri. These cortical signal changes correspond anatomically to the prominent cognitive features of memory loss and frontal executive dysfunction seen in prion diseases,[29] although subcortical circuits are likely to be involved. We found not only that these cortical regions were most commonly involved with the highest SI at baseline but also that these regions all showed an increase in the extent and degree of SI over time. The degree of SI in the left frontal cortex correlated with the degree of spongiosis.

An increase in the extent of cortical signal abnormality with disease progression has previously been reported in sCJD.[9-11] Among 6 patients in whom DWI signal abnormality was seen in the cortex on an early scan, the cortical signal in 2 of the patients progressed from asymmetrical to symmetrical abnormalities on follow-up study.[11] In another single case report, cortical signal abnormality progressed from cingulate, calcarine, and left temporal cortex involvement to also include the left temporoparietal cortex on follow-up study 3 months later.[10] We have not only shown an increase on average in the extent of cortical signal abnormality as the disease progresses in a large cohort of patients with sCJD, but we also describe an increase in the degree of SI in specific cortical brain regions, with the inferior frontal gyrus being the cortical region showing the largest increase in SI in follow-up studies. We have also shown that in a subgroup of patients the left frontal cortical SI correlates with the degree of spongiosis, in line with previous studies.[26,30,31] The combination of an increase in the extent and degree of SI, as captured in a total brain score, correlates with disease duration and is likely to reflect increased spongiform degeneration as CJD progresses.

Most patients herein had an increase in total brain score on follow-up MRI, but we observed a decrease in total brain score in 8 of our patients. The decrease was owing to decreased cortical SI but not subcortical SI, and the areas that showed the greatest decrease were the left inferior tem-

poral gyrus and the right lingual gyrus. The disappearance or decreased conspicuity of DWI cortical signal has been previously reported in the literature and was attributed anecdotally to increased atrophy at the end stage of CJD.[10,11] Our observations herein in a larger cohort of patients confirm the dynamic nature of the cortical DWI signal abnormality in sCJD. We noted a slightly higher atrophy score on follow-up MRI study in patients in whom cortical signal abnormality decreased, which did not reach statistical significance, possibly because of the few patients in the cohort. It is likely that as the disease progresses, neuronal death and loss cause augmentation of the extracellular space, with increased diffusion and decreased DWI signal abnormality before there is frank atrophy.

Among 8 patients with decreased cortical signal abnormality at follow-up, we also found a higher proportion of patients who were heterozygous at codon 129 MV. Although the numbers are small and this finding needs to be confirmed in a larger cohort, it is known that patterns of MRI signal abnormality in sCJD are influenced by codon 129 MV polymorphism status.[7] Therefore, it is possible that the evolution of signal abnormality is also influenced by codon 129 MV polymorphism status, reflecting the known longer disease duration.[32]

Limitations of the study include the subjective nature of the semiquantitative MRI analysis, MRI studies performed on different MRI systems that differed in scan parameters and field strength, and the fact that the MRI readers had knowledge of the clinical diagnosis of sCJD in all patients. All images were viewed on an off-line workstation with appropriate windowing to limit these variables. The few patients included in the quantitative histopathological analysis is also a potential limitation. The study needs to be repeated in a larger cohort with more extensive quantitative histopathological analysis and MRI correlation.

Conclusions

Patients with sCJD show an increase in the extent and degree of signal abnormality in cortical and subcortical regions that correlates with disease duration and the degree of spongiosis. Although cortical signal abnormality may fluctuate, an increase in basal ganglia SI was a consistent finding that was due to an increase in restriction of diffusion. Diffusion abnormalities in the basal ganglia in sCJD may provide a noninvasive biomarker of disease severity for future therapeutic trials that needs to be confirmed in larger studies.

ARTICLE INFORMATION

Accepted for Publication: September 1, 2015.

Published Online: November 16, 2015. doi:10.1001/jamaneurol.2015.3159.

Author Contributions: Dr Hyare had full access to all the data in the study and takes responsibility for the integrity of the data and the accuracy of the data analysis.
Study concept and design: Mead, Jäger, Hyare.
Acquisition, analysis, or interpretation of data: Eisenmenger, Porter, Carswell, Thompson, Mead, Rudge, Collinge, Brandner, Hyare.
Drafting of the manuscript: Eisenmenger, Mead, Jäger, Hyare.
Critical revision of the manuscript for important intellectual content: Rudge, Collinge, Brandner, Jäger.

Conflict of Interest Disclosures: Dr Collinge reported serving on the editorial boards of *Neurobiology of Disease*, *Journal of Neurobiology*, and *Neurogenetics and Neurodegenerative Disease Management*; reported being a director and shareholder of D-Gen Ltd, an academic spin-off company in the field of prion disease diagnosis, decontamination, and therapeutics; and reported receiving research support from the United Kingdom Medical Research Council, the National Institute for Health Research (England), and The Wolfson Foundation. No other disclosures were reported.

Funding/Support: This work was supported by the Department of Health (England) through funding of the National Prion Monitoring Cohort. Some of this work was undertaken at University College London Hospitals/University College London, which received a proportion of funding from the National Institute for Health Research Comprehensive Biomedical Research Centres.

Role of the Funder/Sponsor: The funding sources had no role in the design and conduct of the study; collection, management, analysis, or interpretation of the data; preparation review, or approval of the manuscript; and decision to submit the manuscript for publication.

Additional Contributions: Zane Jaunmuktane, PhD (Department of Neuropathology, National Hospital Queen Square, University College London Hospitals National Health Service Trust), contributed to the study.

REFERENCES

1. Kallenberg K, Schulz-Schaeffer WJ, Jastrow U, et al. Creutzfeldt-Jakob disease: comparative analysis of MR imaging sequences. *AJNR Am J Neuroradiol*. 2006;27(7):1459-1462.

2. Young GS, Geschwind MD, Fischbein NJ, et al. Diffusion-weighted and fluid-attenuated inversion recovery imaging in Creutzfeldt-Jakob disease: high sensitivity and specificity for diagnosis. *AJNR Am J Neuroradiol*. 2005;26(6):1551-1562.

3. Tschampa HJ, Kallenberg K, Kretzschmar HA, et al. Pattern of cortical changes in sporadic Creutzfeldt-Jakob disease. *AJNR Am J Neuroradiol*. 2007;28(6):1114-1118.

4. Kropp S, Finkenstaedt M, Zerr I, Schröter A, Poser S. Diffusion-weighted MRI in patients with Creutzfeldt-Jakob disease [in German]. *Nervenarzt*. 2000;71(2):91-95.

5. Shiga Y, Miyazawa K, Sato S, et al. Diffusion-weighted MRI abnormalities as an early diagnostic marker for Creutzfeldt-Jakob disease. *Neurology*. 2004;63(3):443-449.

6. Matoba M, Tonami H, Miyaji H, Yokota H, Yamamoto I. Creutzfeldt-Jakob disease: serial changes on diffusion-weighted MRI. *J Comput Assist Tomogr*. 2001;25(2):274-277.

7. Fukushima R, Shiga Y, Nakamura M, Fujimori J, Kitamoto T, Yoshida Y. MRI characteristics of sporadic CJD with valine homozygosity at codon 129 of the prion protein gene and PrP^{Sc} type 2 in Japan. *J Neurol Neurosurg Psychiatry*. 2004;75(3):485-487.

8. Hamaguchi T, Kitamoto T, Sato T, et al. Clinical diagnosis of MM2-type sporadic Creutzfeldt-Jakob disease. *Neurology*. 2005;64(4):643-648.

9. Murata T, Shiga Y, Higano S, Takahashi S, Mugikura S. Conspicuity and evolution of lesions in Creutzfeldt-Jakob disease at diffusion-weighted imaging. *AJNR Am J Neuroradiol*. 2002;23(7):1164-1172.

10. Tribl GG, Strasser G, Zeitlhofer J, et al. Sequential MRI in a case of Creutzfeldt-Jakob disease. *Neuroradiology*. 2002;44(3):223-226.

11. Ukisu R, Kushihashi T, Kitanosono T, et al. Serial diffusion-weighted MRI of Creutzfeldt-Jakob disease. *AJR Am J Roentgenol*. 2005;184(2):560-566.

12. Tschampa HJ, Mürtz P, Flacke S, Paus S, Schild HH, Urbach H. Thalamic involvement in sporadic Creutzfeldt-Jakob disease: a diffusion-weighted MR imaging study. *AJNR Am J Neuroradiol*. 2003;24(5):908-915.

13. Collinge J, Gorham M, Hudson F, et al. Safety and efficacy of quinacrine in human prion disease (PRION-1 study): a patient-preference trial. *Lancet Neurol*. 2009;8(4):334-344.

14. Thompson AG, Lowe J, Fox Z, et al. The Medical Research Council Prion Disease Rating Scale: a new outcome measure for prion disease therapeutic trials developed and validated using systematic observational studies. *Brain*. 2013;136(pt 4):1116-1127.

15. Zerr I, Kallenberg K, Summers DM, et al. Updated clinical diagnostic criteria for sporadic Creutzfeldt-Jakob disease. *Brain*. 2009;132(pt 10):2659-2668.

16. Vitali P, Maccagnano E, Caverzasi E, et al. Diffusion-weighted MRI hyperintensity patterns differentiate CJD from other rapid dementias. *Neurology*. 2011;76(20):1711-1719.

17. Scheltens P, Launer LJ, Barkhof F, Weinstein HC, van Gool WA. Visual assessment of medial temporal lobe atrophy on magnetic resonance imaging: interobserver reliability. *J Neurol*. 1995;242(9):557-560.

18. Koedam EL, Lehmann M, van der Flier WM, et al. Visual assessment of posterior atrophy development of a MRI rating scale. *Eur Radiol*. 2011;21(12):2618-2625.

19. Stejskal EO, Tanner JE. Spin diffusion measurements: spin echoes in the presence of a time dependent field gradient. *J Chem Phys*. 1965;42:288-292.

20. Meissner B, Kallenberg K, Sanchez-Juan P, et al. Isolated cortical signal increase on MR imaging as a frequent lesion pattern in sporadic Creutzfeldt-Jakob disease. *AJNR Am J Neuroradiol*. 2008;29(8):1519-1524.

21. Kim JH, Choi BS, Jung C, Chang Y, Kim S. Diffusion-weighted imaging and magnetic resonance spectroscopy of sporadic Creutzfeldt-Jakob disease: correlation with clinical course. *Neuroradiology*. 2011;53(12):939-945.

22. Yi SH, Park KC, Yoon SS, Kim EJ, Shin WC. Relationship between clinical course and diffusion-weighted MRI findings in sCJD. *Neurol Sci*. 2008;29(4):251-255.

23. Aguzzi A, Weissmann C. Prion diseases. *Haemophilia*. 1998;4(4):619-627.

24. Lin YR, Young GS, Chen NK, Dillon WP, Wong S. Creutzfeldt-Jakob disease involvement of Rolandic cortex: a quantitative apparent diffusion coefficient evaluation. *AJNR Am J Neuroradiol*. 2006;27(8):1755-1759.

25. Hyare H, Thornton J, Stevens J, et al. High-b-value diffusion MR imaging and basal nuclei apparent diffusion coefficient measurements in variant and sporadic Creutzfeldt-Jakob disease. *AJNR Am J Neuroradiol*. 2010;31(3):521-526.

26. Caverzasi E, Henry RG, Vitali P, et al. Application of quantitative DTI metrics in sporadic CJD. *Neuroimage Clin*. 2014;4:426-435.

27. Mittal S, Farmer P, Kalina P, Kingsley PB, Halperin J. Correlation of diffusion-weighted magnetic resonance imaging with neuropathology in Creutzfeldt-Jakob disease. *Arch Neurol*. 2002;59(1):128-134.

28. Manners DN, Parchi P, Tonon C, et al. Pathologic correlates of diffusion MRI changes in Creutzfeldt-Jakob disease. *Neurology*. 2009;72(16):1425-1431.

29. Cordery RJ, Alner K, Cipolotti L, et al. The neuropsychology of variant CJD: a comparative study with inherited and sporadic forms of prion disease. *J Neurol Neurosurg Psychiatry*. 2005;76(3):330-336.

30. Lim CC, Tan K, Verma KK, Yin H, Venketasubramanian N. Combined diffusion-weighted and spectroscopic MR imaging in Creutzfeldt-Jakob disease. *Magn Reson Imaging*. 2004;22(5):625-629.

31. Russmann H, Vingerhoets F, Miklossy J, et al. Sporadic Creutzfeldt-Jakob disease: a comparison of pathological findings and diffusion weighted imaging. *J Neurol*. 2005;252(3):338-342.

32. Mead S, Whitfield J, Poulter M, et al. Genetic susceptibility, evolution and the kuru epidemic. *Philos Trans R Soc Lond B Biol Sci*. 2008;363(1510):3741-3746.